Wave phase conjugation under strong fluctuations and consecutive phasing in adaptive optics

V.A. Tartakovsky,[1] V.A. Sennikov,[2] P.A. Konyaev,[2] and V.P. Lukin[2]

[1] Institute of Optical Monitoring, Siberian Branch of the Russian Academy of Sciences, Tomsk
[2] Institute of Atmospheric Optics, Siberian Branch of the Russian Academy of Sciences, Tomsk

Received July 8, 2002

Peculiarities of laser beam propagation with phase conjugation in turbulent medium under strong fluctuations are numerically investigated. The contrast gain is found connected with the appearance of zero-intensity points. It is proposed to measure a light wave phase on spatiotemporal trajectory at those aperture points, where intensity is significant and to determine boundaries of probable optical vortices, i.e., zones where intensity vanishes. Principles of operation and block diagrams are described of two new wave front meters, Hartmann scanning sensor and directional shear interferometer.

Introduction

In adaptive optics, illuminating an adaptive mirror with a wave having simple shape, for instance, a Gaussian wave forms a backward wave. This mirror reproduces phase measured with a wave front sensor. This phase ceases to be a continuous function of two variables when optical vortices localized around zero-intensity points appear in the measurement plane. The optical vortex phase is not determined at a zero point and it is screw-like in its vicinity but the wave amplitude there is small therefore the vortex cannot influence the wave as a whole. However, the backward wave really formed has significant amplitude over the entire adaptive mirror that leads to inadequate increase in the vortex influence and bring in an error in the system operation.

Numerical investigation into optical radiation propagation through ground layer of the turbulent atmosphere along horizontal paths has made the conditions clear for the appearance of deep fading wave parts having zeros of intensity. The results are presented in Section 1. In Section 2 a possibility of measuring phase function on spatiotemporal trajectory is validated. Further, in Sections 3 and 4, two engineering solutions are presented that illustrate feasibility of such measurements. The main results are presented in conclusion.

1. Numerical investigation into propagation and phase conjugation of Gaussian beams in a turbulent medium

In numerical experiment a collimated Gaussian beam, being a reference radiation source, with the initially plane phase propagated through randomly inhomogeneous medium, experienced phase conjugation in the plane of an adaptive mirror, and came back. Figure 1 shows schematically the model of the experiment.

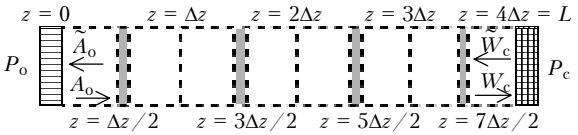

Fig. 1. Schematic model of the experiment on phase conjugation of a Gaussian beam propagated through a turbulent medium. P_o is the object plane; P_c is the adaptive mirror plane. A number of phase screens is four (shown by gray color), grid matrix rank is 512, the ratio between the outer and inner scales is $L_0/l_0 = 10^3$.

The calculations have been done using a well known numerical model.[1,2] The dimensionless parabolic quasi-optical equation have been solved in paraxial approximation in the form

$$\frac{\partial W}{\partial z} = \frac{i}{2}\left(\frac{\partial^2}{\partial x^2} + \frac{\partial^2}{\partial y^2} + T\right) W, \qquad (1)$$

where $W(x, y, z)$ is normalized complex amplitude of the wave; T is the temperature field with the spectral density

$$F(\kappa_x,\kappa_y) = C_T^2\,(\kappa_0^2 + \kappa_x^2 + \kappa_y^2)^{-11/6}\,\exp\,[-(\kappa_x^2 + \kappa_y^2)/\kappa_m^2],$$

$$\kappa_0 = 2\pi/L_0, \quad \kappa_m = 2\pi/l_0. \qquad (2)$$

In this equation κ_x and κ_y are spatial frequencies; L_0 and l_0 are the outer and the inner scales of turbulence normalized to the beam radius a_0, in the experiment the former ones were 100 and 0.1 cm, respectively. The wave parameter $z_0 = \lambda L/2\pi a_0^2$ was equal to 0.1 for wavelength $\lambda = 0.63$ μm. The values of all parameters are characteristic of a horizontal path with the length $L = 1$ km in the ground layer of turbulent atmosphere, the beam radius being $a_0 = 10$ cm.

0235-6880/02/12 1002-09 $02.00

Two-cycle scheme of the splitting method has been used. The number of steps on the path were four, the grid matrix rank was equal to 512. The Monte Carlo method has been used; estimates have been calculated as a mean over 200 realizations.

Influence of turbulence on the beam was characterized by scintillation index σ_I^2, that is a normalized variance of fluctuations of the Gaussian beam intensity I calculated on the beam axis. The dependence of σ_I^2, on temperature structure characteristics C_T^2 is presented in Fig. 2.

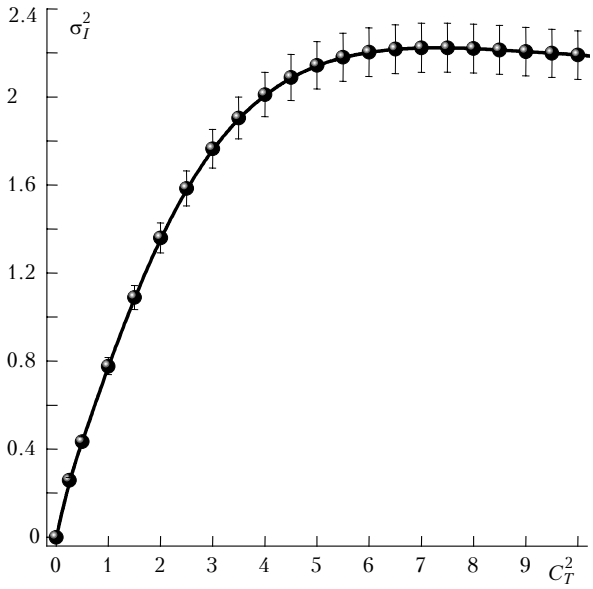

Fig. 2. Dependence of scintillation index σ_I^2 on temperature structure characteristics C_T^2, obtained in the numerical experiment. Estimations were calculated as a mean over 200 realizations. Root-mean-square deviations are shown by bars.

Figure 3 presents distributions of intensity and phase of the Gaussian beam after passing through the turbulent medium at various values of scintillation index σ_I^2, corresponding to both week, $\sigma_I^2 < 1$, and strong, $\sigma_I^2 > 1$, turbulence. It is seen that under strong turbulence the beam experiences significant amplitude-phase fluctuations. The beam intensity has strongly pronounced peaks that are several times greater than the initial Gaussian beam maximum. In the central part of the beam there appear areas with deep intensity fading where the appearance of zero intensity surrounded by optical vortices is possible.

When considering energy transfer through the atmosphere, we will believe that light wave propagation in the medium and in the optical system channels, between object plane P_o and adaptive mirror plane P_c, is a linear integral transform. With all this going on, the reciprocity principle holds and the energy is conserved. The following relations can present these features:

$$W_c(\mathbf{r}_c) = \iint_{P_o} h(\mathbf{r}_o, \mathbf{r}_c)\, W_o(\mathbf{r}_o)\mathrm{d}\mathbf{r}_o,$$
$$W_o(\mathbf{r}_o) = \iint_{P_c} h(\mathbf{r}_o, \mathbf{r}_c)\, W(\mathbf{r}_c)\mathrm{d}\mathbf{r}_c; \qquad (3)$$
$$\iint_{P_o} \left| W_o(\mathbf{r}_o)\right|^2 \mathrm{d}\mathbf{r}_o = \iint_{P_c} \left| W_c(\mathbf{r}_c)\right|^2 \mathrm{d}\mathbf{r}_c.$$

Here function $h(\mathbf{r}_o, \mathbf{r}_c) = h(x_o, y_o, x_c, y_c)$ is the pulse response. Since the reciprocity principle holds in the turbulent medium, this function does not depend on propagation direction between P_o and P_c planes.[3]

Interrelation between the input and output errors is among most important characteristics of the system. When deriving expressions for calculation of errors, we have taken into account Eqs. (3) (see Ref. 4), from which it follows that square norm of difference between complex functions

$$\iint_{P_o} \left| W_o(\mathbf{r}_o) - \tilde{W}_o(\mathbf{r}_o)\right|^2 \mathrm{d}\mathbf{r}_o =$$
$$= \iint_{P_c} \left| W_c(\mathbf{r}_c) - \tilde{W}_c(\mathbf{r}_c)\right|^2 \mathrm{d}\mathbf{r}_c \qquad (4)$$

keeps as the wave propagates in the system under consideration.

In Eq. (4) the function $\tilde{W}_c(\mathbf{r}_c)$ characterizes the modified wave formed on the adaptive mirror. In this connection we believe that $W_c(\mathbf{r}_c)$ provides maximum effect when the reciprocity principle is realized. The function $\tilde{W}_o(\mathbf{r}_o)$, in its turn, is a wave that was formed in the object plane as a result of propagation of the modified wave $\tilde{W}_c(\mathbf{r}_c)$ from P_c to P_o plane. Modification does not exist at complete phase conjugation therefore both parts of the Eq. (4) vanish.

The input error is calculated on the adaptive mirror at the plane where the backward wave P_c is formed. It is expedient to hold in this error the influence of all wave constituents. Towards this end we determine the error as a relation of square norms

$$\varepsilon_c = \sqrt{\iint_{P_c} \left| W_c(\mathbf{r}_c) - \tilde{W}_c(\mathbf{r}_c)\right|^2 \mathrm{d}\mathbf{r}_c \Big/ \iint_{P_c} \left| W_c(\mathbf{r}_c)\right|^2 \mathrm{d}\mathbf{r}_c}. \qquad (5)$$

The error (5) depends on the wave phase therefore it is not suitable for characteristics of image formation quality or focusing. As such operations do not require the phase to be held, it is expedient to calculate the root-mean-square deviation of the amplitude of a phase-conjugated wave $\tilde{A}_o$ from the object amplitude A_o at the plane P_o.

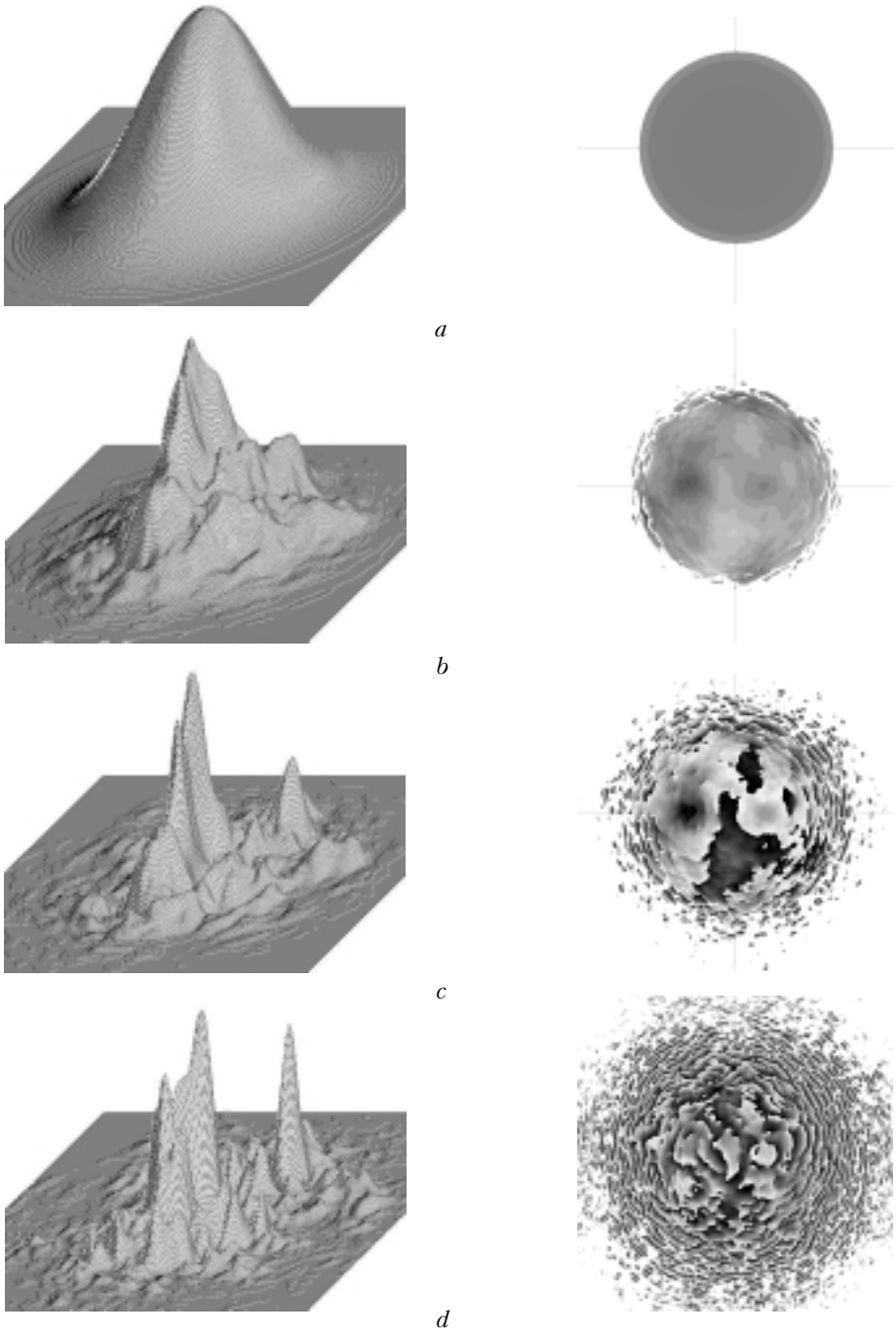

Fig. 3. Intensity (on the left) and phase (on the right) of a Gaussian beam after passing turbulent medium with different values of the parameter $C_T^2 = 0$, 0.1, 1, and 5 (*a, b, c,* and *d*).

This error characterizes the results of the system effect in other words it is the output error:

$$\varepsilon_o = \sqrt{\iint\limits_{A_o} [A_o(\mathbf{r}_o) - \tilde{A}_o(\mathbf{r}_o)]^2 \, d\mathbf{r}_o \Big/ \iint\limits_{A_o} A_o^2(\mathbf{r}_o) d\mathbf{r}_o}. \qquad (6)$$

It is obvious that in the case the ratio between ε_o and ε_c will not be linear, as in Eq. (4), for all types of modifications of the phase conjugated wave, but at small ε_c the linearity holds. In the general case, the interrelation is monotonic.[4]

In the numerical experiment we have studied behavior of $\varepsilon_o(C_T^2)$ that is one of two modification methods (amplitude and phase) proposed in Ref. 4. The amplitude modification consists in zeroing those wave parts on the aperture that have amplitude lower than a preset threshold. Phase modification of the phase-conjugated wave consisted in that the wave phase in the parts where the amplitude was lower than the preset threshold has been substituted for constant value or some periodic function that removes these wave parts

from the propagation channel. In so doing the wave amplitude has been kept unchanged.

The threshold value ΔA has been chosen as fractions of the maximum amplitude of a Gaussian beam. An estimate of ε_o value was calculated as a mean over 200 realizations within circle having radius four times greater than the initial beam radius. All modification methods yielded practically similar results. It was found that there are two different behavior types of $\varepsilon_o(C_T^2)$. They are presented in Fig. 4.

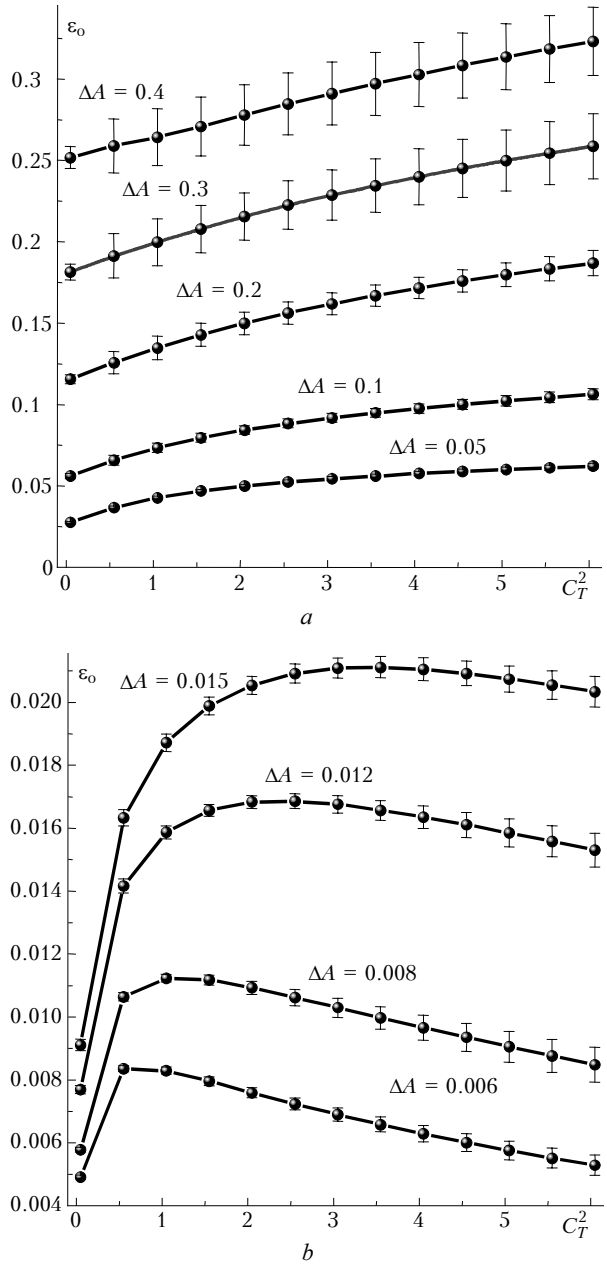

Fig. 4. Dependence of phase conjugation error ε_o on the parameter C_T^2 at the amplitude threshold value $\Delta A = 0.05$; 0.1; 0.2; 0.3; 0.4 (*a*) and $\Delta A = 0.006$; 0.008; 0.012; 0.015 (*b*). The estimates have been calculated as a mean over 200 realizations. Root-mean-square deviation is shown by vertical bars.

Sallow local intensity minima and low maxima turn out to be lower than the threshold at $\Delta A > 0.05$. It is obvious that in such domains the energy may increase as the turbulence increase, therefore ε_o monotonically grows as well. This increase should likely stop and the curves in Fig. 4*a* will reach their saturation at a stronger turbulence, but such turbulent fluctuations have not been studied yet.

At $\Delta A < 0.02$, ε_o, first, increases, reaches its maximum, and then smoothly decreases. Such dependence can be explained by the fact that turbulence intensification in the medium is accompanied by deepening of the local minima and their consequent conversion into zero-intensity points. Zero-intensity points formed differ qualitatively from other points on the aperture because an optical vortex is localized around them. An energy flux in the vortex has outward constituents. As a result, the wave energy goes out from a zero point that, probably, facilitates its steadiness. The appearance of a zero is a discrete event. Accumulation of such events along with strengthening of fluctuations results in that the intensity is no longer lower than the preset threshold. As a result, the phase conjugation error ε_o stops to grow and begins to gradually decrease. This explains the presence of maximum in Fig. 4*b*.

It is known from field experiments,[5] that when propagating through the turbulent medium, laser beam, being in the area of strong fluctuations, disintegrates into separate radiation filaments, whose cross size weakly depends on the path length. The numerical experiment performed has revealed the initial stage of forming such filaments. It is characterized by disappearance of the beam parts where the energy is lower than the preset threshold and by the beam contrast expansion.

Thus, the error ε_o, arising when wave parts with the amplitude lower than the preset threshold are removed from the adaptive system channel, grows rather slowly as the fluctuations increase and it has some limits. It shows that as turbulence increases some domains are formed containing insignificant energy, whereas the main portion of the wave energy is localized in filaments (see Fig. 3). The phase within each of the filaments is a continuous function by definition.

Phase ceases to be continuous function of two variables in the aperture parts where energy is insignificant when points with zero intensity appear. However it can be continuous function on the trajectory lying in the aperture plane. The trajectory should fill the filaments' domains with the necessary density and connect these domains going around a zero point. In those domains where existence of optical vortices is possible, there is no need to measure phase it is enough to determine only their boundaries.

When an ordinary multichannel wave front sensor with parallel information detection is used, a computer can realize numerical methods of phase reconstruction along the considered trajectory. But parallel measurements themselves are not needed. It is necessary only to minimize ε_c, i.e., difference between the phase-

conjugated wave and the wave required for total compensation in accordance with the reciprocity principle. Therefore it is possible to consider scanning of the aperture to be measured by single-channel wave front sensor, consequent calculations, and phasing of the adaptive mirror elements. In this case time will be a trajectory parameter over all interval of the system operation.

Scanning gives a possibility of realizing in an adaptive system a definite strategy, namely, aperture domains having higher intensity should be measured more accurately and inverted with less delay as compared to those domains where light intensity is small.[6] This is the preference over the parallel signal processing.

Beyond the problems of optical vortices, other possibilities appear during scanning. In particular, it is very suitable to apply Fast Fourier Transform (FFT), intended for periodic functions, for analysis of continuous functions determined on a closed path. This algorithm has high speed and allows one to reduce the problem to optimal filtration of functions of the trajectory parameter, at the same time no edge effects arise.[7]

Finally, when scanning function of two variables, it is possible to get statistically independent realizations determined on the orthogonal trajectories. They are necessary, for example, for calculating average values or determining *a posteriori* error of the phase reconstructed.[8]

Below we shall justify a possibility of measuring light wave phase on the trajectory in the aperture plane and consider schematic models of two scanning sensors – diffraction and interference ones.

2. Phase determination along the trajectory

It is necessary to give a non-contradictory definition of a wave process phase. Maxwell equations do not include such definition therefore some supplementary statements are considered. They specify function class determining mathematical model of a wave. There are publications concerning problems on definition of amplitude and phase as applied to one-dimensional oscillation process. Vakman[9,10] and Zolotarev[11] give rather complete bibliography on this problem. Different methods for determination of amplitude and phase are useful in the framework of problems to be solved and mathematical models used, but an analytical signal (AS) introduced by Gabor[12] in 1946 has accepted the widest use. It happened mostly due to efforts by Vakman. When comparing different methods, he took into account continuity and differentiability of the signal amplitude, unit independence of phase, and coincidence with intuitive ideas of amplitude and phase of harmonic functions.

But this problem is not complete. The reason is that there is no uniform approach to construction of mathematical models of oscillations, waves, and signal conversion systems. The algorithms for amplitude and phase determination have been proposed, but there is no explicitness about principal features of both the signal and concepts introduced.

Analysis of a light wave is carried out in the P_c plane of an optical system after its interaction with inhomogeneities. We believe that the medium there is non-conducting, homogeneous, and isotropic. We also believe that in constitutive equations relation between induction and field strength is linear and local for both electric and magnetic fields. Let light polarization be unchanged. At such limitations Maxwell equations are reduced to the wave equation for quasi-monochromatic scalar and real wave $U(x, y, z, t)$ with the constant absolute refractive index. The solution of this equation can be represented in the form of the triple Fourier integral

$$U(x,y,z,t) = \int_{-\infty}^{\infty}\int_{-\infty}^{\infty}\int_{-\infty}^{\infty} S(\alpha,\beta,\omega)\exp i(\alpha x + \beta y \pm \gamma z + \omega t)\,d\alpha\,d\beta\,d\omega \qquad (7)$$

and it makes sense of scalar wave propagating from the $z = 0$ plane in the opposite directions. Here α and β are spatial frequencies; ω is time frequency; S is spatiotemporal spectrum in the plane orthogonal to the z-axis, i.e., wave propagation direction.

Equation (7) is valid within above assumptions and reduces the problem on light wave propagation in the homogeneous medium to defining the initial conditions for the spectrum. The spectrum $S(\alpha, \beta, \omega)$ can be defined as two-dimensional Fourier transform with respect to x and y of the wave given in Kirchhoff approximation. According to this approximation, in the recording plane a wave scattered by an object is prescribed within the optical system aperture, while outside the aperture it is supposed to be zero. It is very rough approximation and it does not satisfy the wave equation where it was defined. But filtering properties of Eq. (7) at $z \gg \lambda$ result in suppression of the error introduced by Kirchhoff conditions. The plane waves are filtered, while inhomogeneous waves, for which an inequality $k^2 < \alpha^2 + \beta^2$ is valid, decay exponentially.

Scalar approximation need in considering the problems in parabolic approximation, where $k^2 \gg \alpha^2 + \beta^2$, $\gamma \approx k - (\alpha^2 + \beta^2)/2k$ with a narrow spatial frequency spectrum, $\Delta\alpha/\alpha_c < 1$, α_c is the carrier frequency, $\Delta\alpha$ is a halfwidth of the spatial frequency spectrum. Besides, it is known *a priori* that relative time spectrum width of the quasi-monochromatic wave $U(x, y, z, t)$ is very small, $\Delta\omega/\omega_c < 1$, ω_c is the carrier frequency, $\Delta\omega$ is time spectrum halfwidth. These are the physical grounds for the assumption on the spectra finiteness, so the integration limits in Eq. (7) will be finite quantities.

The light wave properties under consideration can be expressed most naturally if $U(x, y, z, t)$ is an integer function of exponential type for every variable. This means that physical characteristics (quasi-

monochromaticity and parabolic behavior) are superimposed on the approximation of $U(x, y, z, t)$ wave. The approximation is a solution of another task; at least it has no inhomogeneous values, whereas it will be a part of the amplitude and phase concepts that do not result from the wave equation.

Let us apply the definition of analytical signal with respect to variable t, which consists in providing time spectrum causality, to the real function (7) and obtain an analytical signal as a specific solution of the scalar wave equation that corresponds to quasi-monochromatic wave propagating in homogeneous medium in positive direction of the z-axis

$$W(x, y, z, t) = U(x, y, z, t) + iV(x, y, z, t) =$$

$$= \int_0^\infty d\omega \int_{-\infty}^{\infty}\int_{-\infty}^{\infty} S(\alpha,\beta,\omega) \exp i(\alpha x + \beta y + \gamma z - \omega t)\, d\alpha d\beta. \quad (8)$$

The sign of the spatial frequency γ was chosen such that inhomogeneous waves decay at $z \to +\infty$, and of the frequency ω – such that wave front moves in the same direction. The frequency ω, as well as γ, does not change the sign, so the function $W(x, y, z, t)$ is an analytical signal not only with respect to variable t, but also with respect variable z.

It follows from Eq. (8) that such fundamental light properties as spatial and time coherence, as well as the fact whether it is monochromatic or white, are connected with spectrum width $S(\alpha, \beta, \omega)$ of the analytical signal $W(x, y, z, t)$.

Let parametric equations for line $l(t)$ on the plane are given:

$$x = x_o + tv_x(t), \quad y = y_o + tv_y(t), \quad z = z_o. \quad (9)$$

Let us clarify under which conditions the wave will be an analytical signal on this line. Substituting the parametric equations into Eq. (8), we obtain

$$W[l(t)] = \int_0^\infty d\omega \int_{-\infty}^{\infty}\int_{-\infty}^{\infty} S(\alpha,\beta,\omega) \times$$

$$\times \exp i[(\omega_s - \omega)\, t + \varphi_o]\, d\alpha d\beta, \quad (10)$$

where

$$\omega_s = \alpha\, v_x(t) + \beta\, v_y(t); \quad \varphi_o = \alpha\, x_o + \beta\, y_o + \gamma\, z_o.$$

Denote the largest width of the spatial spectrum carrier as $\eta = \max(|\alpha|, |\beta|)$ and maximum speed of the aperture scanning as $v = \max(|v_x(t)|, |v_y(t)|)$. Then we find that $\max|\omega_s| < 2\eta v$. Let us consider the value

$$q = 2v\eta/\omega_c = \sqrt{2}\, v \sin\theta / c < 1,$$

where θ is maximum angle between the wave vector and recording plane. Numerical estimates made for q in the frequency interval $(\omega_c \pm \Delta\omega)$ at $\Delta\omega/\omega_c \gg 1$ show that inequality $\omega_s - \omega_c < 0$ is valid at practically important values of the parameters η and v. Thus, the factor at the variable t in Eq. (10) does not change its sign and function $W[l(t)]$ is an analytical signal on the line with parameter t.

Analytical signal (10) is a section of the function $W(x, y, z, t)$ [Eq. (8)]. Therefore the amplitude and phase of this signal are sections of $|W(x, y, z, t)|$ and $\arg W(x, y, z, t)$ that are functions of four variables. It is clear that this property is a consequence of the fact that time and spatial spectra connected with wave propagation direction are narrow-band. An optical wave in quasi-monochromatic and parabolic approximations has these properties. Besides, when spatial coordinates and time enter the exponent (Eq. (8)) as additive parts, the structure of the wave equation solution allows one to use in analysis both spatial and time carriers simultaneously.

Practical importance of Eq. (10) is that it gives a possibility of synthesizing algorithms for phase measurements in different spatiotemporal, one- and multidimensional sections and provides its coincidence in these sections with the only phase that is the function of four variables.

Let us present the function of phase in the aperture plane in the ordinary form

$$\varphi(x, y) = \arctan \frac{V(x, y)}{U(x, y)} \quad (11)$$

and consider its partial derivatives with respect to x and y variables

$$\varphi'_x = \frac{V'_x U - U'_x V}{A^2}, \quad \varphi'_y = \frac{V'_y U - U'_y V}{A^2};$$

$$A^2 = U^2 + V^2. \quad (12)$$

Considering the wave function $W(x, y) = U(x, y) + iV(x, y)$ as a function with finite Fourier transform with respect to all variables, one can draw a conclusion that partial derivatives of phase, including the higher order ones, exist and they are continuous at all points, where $A(x, y) \neq 0$. The function of phase can be determined by a curvilinear integral of total differential over a trajectory with parameter p, lying in xy plane

$$\varphi(x,y) = \int_0^{(x,y)} \left(\varphi'_x dx + \varphi'_y dy\right) = \int_0^p \frac{d\varphi}{dp} dp, \quad (13)$$

where

$$\begin{cases} x = x(p) \\ y = y(p) \end{cases}$$

are parametric equations.

If the trajectory does not traverse zero points and does not cross sections going from zero points outside the integration domain, the integral is trajectory-independent in such a simply connected domain. The phase function is continuous and single-valued on such a trajectory. This property will allow an arbitrarily dense filling of the plane under study with this trajectory.

3. Hartmann scanning sensor

Hartmann method is applied for testing telescope optics. The method is based on measurement of focal spots' position. Descartes and Lomonosov knew this method. Vitrichenko in Ref. 13 described classical version of this method in detail, where one can find complete bibliography on this problem. The so-called Shack–Hartmann Test[14] is the further development of the method. In this test small lenses or prisms are used in every sub-aperture instead of a diaphragm in its classical version. It makes the optical layout more compact and admits variations in focal spot sizes and their displacement.

The Hartmann sensor uses interrelation between coordinates of sub-aperture spot center of gravity and wave phase derivative in this sub-aperture. Let us consider the first moment m_1 of the squared modulus of Fourier transform $|S(\alpha)|^2$. Applying the moment theorem and Parseval formula to function $W(x, y) = A(x, y)\exp i\varphi(x, y)$ and omitting y coordinate, we obtain

$$m_1 = \int_{-\infty}^{\infty} \alpha |S(\alpha)|^2 \mathrm{d}\alpha =$$

$$= \frac{i}{2\pi}\left[\frac{\mathrm{d}}{\mathrm{d}x}\int_{-\infty}^{\infty} W(\eta)\, W^*(\eta - x)\mathrm{d}\eta\right]_{x=0} =$$

$$= -\frac{1}{2\pi}\int_{-\infty}^{\infty} A^2(x)\,\varphi'(x)\mathrm{d}x + \frac{i}{4\pi}[A^2(\infty) - A^2(-\infty)]. \qquad (14)$$

Imaginary part of this equation should be equal to zero based on condition that the squared modulus of function $W(x)$ should be integrable over all x axis.

Normalizing Eq. (14), we obtain an expression that relates the coordinate of focal spot center of gravity and phase derivative

$$\alpha_c = \frac{\int_{-\infty-\infty}^{\infty\ \infty} \alpha |S(\alpha,\beta)|^2 \mathrm{d}\alpha\,\mathrm{d}\beta}{\int_{-\infty-\infty}^{\infty\ \infty} |S(\alpha,\beta)|^2 \mathrm{d}\alpha\,\mathrm{d}\beta} =$$

$$= -\frac{\iint_G A^2(x,y)\,\varphi'_x(x,y)\mathrm{d}x\mathrm{d}y}{\iint_G A^2(x,y)\,\mathrm{d}x\mathrm{d}y}, \qquad (15)$$

where G is a sub-aperture domain in Hartmann diaphragm.

It follows from this equation that coordinate of focal spot center of gravity gives the value of phase derivative on the sub-aperture if only the amplitude $A(x, y) = \mathrm{const}$ and phase is planar ($\varphi'_x = \mathrm{const}$, $\varphi'_y = \mathrm{const}$). Otherwise it will be average or weighted mean derivative. These are the method limitations. The sub-aperture size itself makes no sense in this case, but it is obvious that it should be as small as possible. In the atmosphere the scale, on which the constancy and planarity conditions could be considered fulfilled, is determined by the coherence radius r_0 (Ref. 15). Phase difference on the r_0 scale may reach 2π radian that may result in focal spot displacements and larger aperture size, so it will be impossible to distinguish focal spots from different apertures in the ordinary Hartmann scheme.

Applying Shack–Hartmann Test, one can decrease focal spot displacements by means of changing focal length of the sub-aperture lens. But in this case it is necessary to increase sensitivity and decrease a pixel size of the photodetector array. This contradiction can be resolved by means of placing prisms into sub-apertures that increase a distance between fluctuation zones of separate spots.

An improvement of the sensor design that allows one to measure wave phase as a phase of spatiotemporal analytical signal on the trajectory has been suggested in 1996.[6] Block diagram of the sensor is shown in Fig. 5. Since this sensor has only one aperture, relative to which a beam to be measured is scanned, there are no difficulties connected with choosing the number and size of sub-apertures. In scanning, the sub-aperture size may be changed for the purpose of increasing sensitivity and resolution, as well as for meeting conditions of the amplitude constancy and phase planarity more closely. In such a design a range of the focal spot displacement has no principle limitations. It may be more than 9000 λ at wave front root-mean-square measurement error of 0.014 λ. These values are presented in more late paper,[16] where a realization of an idea similar to Hartmann scanning sensor is described.

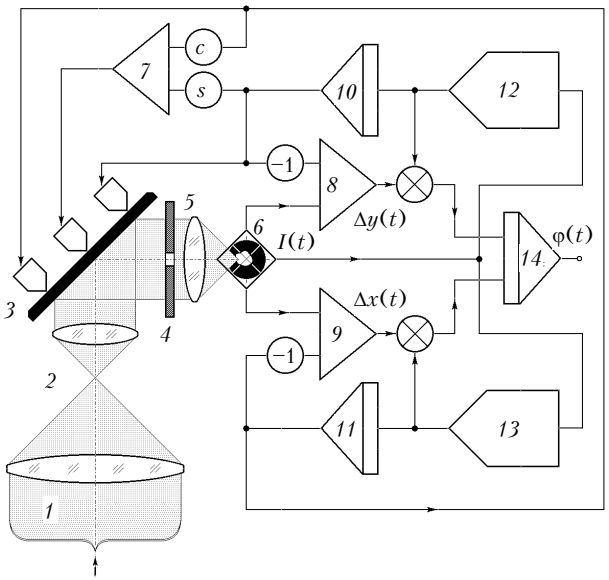

Fig. 5. Hartmann scanning sensor: ( ) multiplying blocks; (○) transmission coefficients.

Principle of operation of the sensor shown in Fig. 5 is based on integration of a total differential (Eq. (13)).

The following operations are performed in the sensor. Light beam *1* after scaling in the input optical system *2* comes to the deflector *3* that scans it along the diaphragm aperture *4*, behind which there is a lens Fourier converter *5*. The converter forms a focal spot on the coordinator *6* that determines abscissa and ordinate of the spot's center of gravity, as well as its integral intensity. The latter enters the blocks *12* and *13* as a feedback signal for the trajectory correction. Processing of the abscissa and ordinate of the focal spot center of gravity is carried out in two channels. The intergrators *8* and *9* contain the difference between coordinates measured in block *6* and the displacements coming from blocks *10* and *11* that determine an inclination of the deflector *3*. Signals proportional to the phase derivatives with respect to x and y coordinates, coming from the outputs of the integrators *8* and *9*, and time derivatives with respect to Cartesian coordinates of the trajectory $x(t)$ and $y(t)$, coming from the blocks *12* and *13*, are multiplied, added up, and integrated in accordance with Eq. (16), in block *14*. The phase $\varphi(t)$, as a function of time, is formed at the output of block *14*. The derivatives of Cartesian coordinates of the trajectory from the blocks *12* and *13*, in its turn, are integrated in blocks *10* and *11*, re-calculated for three-point control using coefficients c and s at the input of block *7*, and enter into three drives of the deflector *3*.

The coordinator is one of the basic elements. The principle of operation for such devices has been described in many papers and it may vary widely. Thus, for example, a displacement sensor has been described[17] with optoelectronics converter. It operates in a follow-up mode and has a feedback to compensate for changes in the focal spot shape and intensity. Another version is a position-sensitive photodetector.

4. Directional shear interferometer

Shearing interferometer can be applied as a wave front sensor. Harmonic phase modulation, two-wave interference, and locked-in detection are used in this interferometer. As compared with Hartmann sensor, selection of optical waves having narrow spectral distribution is possible in an interferometer. Since interference pattern may be considered as a superposition of coherent and incoherent constituents, a coherent component with low spatial frequency is separated out due to interference. It is useful for eliminating background illumination, unpolarized radiation, and high spatial frequencies. Laser radiation source quality, photodetector, filters, and path length in the atmosphere determine the selection efficiency.

Figure 6 presents a directional shear interferometer. It is supposed that the light wave has properties of spatiotemporal analytical signal (Eq. (10)). Unlike known interferometers,[18,19] in the interferometer considered direction of a shear is alternative and coincides with the scanning direction along the aperture under investigation. The scanning allows to bypass deep wave intensity attenuation along spatiotemporal trajectory and to measure wave phase on this trajectory.

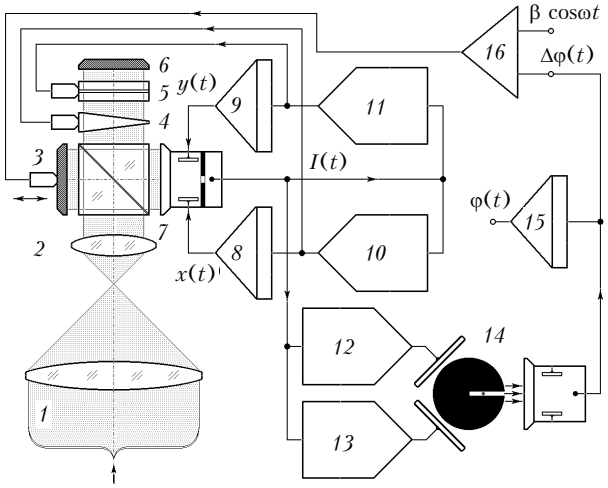

Fig. 6. Directional shear interferometer.

The sensor operates in the following way. Light *1* scattered by an object is converted by the input optics *2*, enters the interferometer where it is split into two beams. A phase modulator *3* inserts harmonic modulation into one of the beams. Another beam passes successively through two elements *4* and *5* that shear the beam along the orthogonal directions across the optical axis. Then, being reflected from the mirror *6*, this beam passes elements *4* and *5* in the backward direction and is superposed with the phase-modulated beam on the beam splitter *3*. In this case the spatiotemporal interference pattern is formed that enters the scanning photodetector *7*.

This interference pattern contains modulated constituent in the form

$$A(x, y, t)\cos[\Delta\varphi(t) + \beta\cos\omega t];\ \ \Delta\varphi(t) =$$

$$= \varphi[x(t) + \Delta x(t), y(t) + \Delta y(t), t] - \varphi[x(t), y(t), t], \quad (16)$$

where β is the modulation coefficient; ω is the circular frequency of modulation; x and y are the spatial coordinates in the photodetector plane *7*; t is time. The signal amplitude $A(t, x, y)$ is proportional to modulus of mutual coherence function. The phase difference $\Delta\varphi(t)$ in these channels will be identical to phase of the mutual coherence function.

Time spectrum of constituent (16) contains lines at the frequencies ω and 2ω:

$$2A(x, y, t)\, J_1(\beta)\sin\Delta\varphi(t)\cos\omega t,$$

$$2A(x, y, t)\, J_2(\beta)\cos\Delta\varphi(t)\cos 2\omega t, \quad (17)$$

Amplitudes of these oscillations can be equalized assuming that $\beta \approx 2.65$, because in the vicinity of this point the Bessel functions are equal to each other, $J_1(2.65) \approx J_2(2.65) \approx 0.45$.

The photodetector *7* scans the interference pattern and the signal from it enters selective filters *12* and *13*, for instance, synchronous detectors, for separating out quadratures at the modulation frequency ω and

doubled frequency, respectively. The quadratures $2A(t)\,J_1(\beta)\,\sin\Delta\varphi(t)$, $2A(t)\,J_2(\beta)\,\cos\Delta\varphi(t)$ are sent from the filter outputs to converter *14* that converts Cartesian coordinates into polar ones. The converter can consist of cathode-ray tube (CRT) with a slit mask and a photodetector. When applying the quadratures to orthogonal CRT inputs, phase fluctuations $\Delta\varphi(t)$ cause azimuth displacements of the spot on the tube screen whereas amplitude fluctuations $A(t)$ cause radial displacements. An opaque mask with narrow radial slit is placed on the tube screen. Light from the spot on the screen is detected by a photodetector. This signal will depend only on $\Delta\varphi(t)$ value that, by means of negative feedback, sums up with harmonic phase modulation signal $b\cos\omega t$ in unit *16* and control displacement of the phase modulator *3*, returning the CRT spot to the slit center. Thus, amplitude and phase modulation are separated out.

Phase difference $\Delta\varphi(t)$ is proportional to the derivative with respect to trajectory parameter, i.e., $d\varphi/dt$ when displacement $\sqrt{\Delta x^2 + \Delta y^2}$ is rather small and constant. This value is integrated over time by unit *15* and the wave phase $\varphi(t)$ is formed at its output as a function of time along the trajectory $x = x(t)$, $y = y(t)$. Trajectory sweeps, when scanning photodetector *7*, are given as derivatives dx/dt and dy/dt in oscillators *10* and *11*. In order to provide scanning that is adaptive to wave intensity, feedback between units *10*, *11*, and photodetector *7* is used in the aperture.

Conclusion

It is most likely that the optical vortices localized around zero-intensity points just cause the disintegration of a laser beam into separate filaments when propagating through the atmosphere. The filaments absorb the main beam energy; domains with low intensity where zero points are located separate them. It is expedient to remove these domains from an adaptive system channel. In any case there is no need to measure phase there, it is quite sufficient to determine position of these domains in the aperture.

In the aperture plane the wave remains a continuous function of two variables even when zero-intensity points appear. The continuity results from the possibility of introducing spatiotemporal analytical signal that is a consequence of the narrow time and spatial spectra connected with direction of wave propagation. The structure of wave equation solution allows one to use both spatial and temporal carriers simultaneously.

Zeros are singular points for phase as a calculated value. Taking into account that zeros are located at isolated points, one can make sections from zeros outside the aperture. Within the simply connected domain formed, it is possible to determine piecewise-smooth trajectory that does not touch section, on which the phase will be a continuous time function in scanning. Since the trajectory is closed, phase will be uniquely determined on this trajectory. In this case wave continuity on the trajectory is provided. The wave can be extended over all apertures from the trajectory points, excluding the section vicinity.

Now when phase is determined at a particular aperture point, it can be fixed on the corresponding element of an adaptive mirror. Mirror phased in such a way will reconstruct a backward wave when a light source is switched on. Particular scanning algorithms can be realized using different methods and different parameters, not obligatorily in time. Wave front scanning sensors, which record a focal spot or a shear interference pattern, can be useful for the development of the element base.

References

1. V.E. Zuev, P.A. Konyaev, and V.P. Lukin, Izv. Vyssh. Uchebn. Zaved., Ser. Fizika **XXVIII**, No. 11, 6–29 (1985).
2. V.P. Lukin, F.Yu. Kanev, P.A. Konyaev, and B.V. Fortes, Atmos. Oceanic Opt. **8**, No. 3, 210–214 (1995).
3. J.H. Shapiro, J. Opt. Soc. Am. **61**, No. 4, 492–495 (1971).
4. N.N. Mayer and V.A. Tartakovsky, Atmos. Oceanic Opt. **8**, No. 12, 1069–1072 (1995).
5. V.Ya. S'edin, S.S. Khmelevtsov, and M.F. Nebol'sin, Izv. Vyssh. Uchebn. Zaved., Ser. Radiofizika **17**, No. 1, 44–49 (1970).
6. V.A. Tartakovsky and V.P. Lukin, in: *Adaptive Optics*, Technical Digest Series **13**, 241–242 (1996).
7. V.A. Tartakovsky, L.V. Barabina, and V.P. Lukin, in: *Propagation of Optical Radiation in Randomly Inhomogeneous Media* (Publishing House of Institute of Atmospheric Optics SB RAS, Tomsk, 1988), pp. 49–55.
8. V.A. Tartakovsky, in: *Fringe Pattern Evaluation and Analytic Signal Theory* (Akademie Verlag, Optical Metrology Series, Berlin, 1997), pp. 84–91.
9. D.E. Vakman, IEEE Trans. Signal Process **44**, No. 4, 791–797 (1996).
10. D.E. Vakman and L.A. Vainshtein, Usp. Fiz. Nauk **123**, Issue 4, 657–682 (1977).
11. I.D. Zolotarev, Tekhn. Radiosvyazi, No. 3, 3–10 (1997).
12. D. Gabor, J. IEE **93**, Pt. 3, 429–441 (1946).
13. E.A. Vitrichenko, V.P. Lukin, L.A. Pushnoy, and V.A. Tartakovsky, *Problems of Optical Control* (Nauka, Novosibirsk, 1990), 351 pp.
14. N.J. Wooder, I. Munro, T.W. Nichols, M. Wells, and J.C. Dainty, in: *Adaptive Optics*, Technical Digest Series **23**, 56–58 (1995).
15. M.C. Roggemann and B. Welsh, *Imaging through Turbulence* (CRC Press, 1966), 336 pp.
16. S. Bucourt and J. Ruhmann, in: *EuroPhotonics* (1999), pp. 36–37.
17. V.L. Simonov, in: *Proceedings of ESO Conference and Workshop on Active and Adaptive Optics* (1993), No. 48, pp. 363–368.
18. O.N. Emaleev, V.V. Nazarchuk, V.V. Pokasov, M.M. Raizman, and L.G. Shoshin, "*The tracing digital phase meter in the optical range*," Inventor's Certificate No. 397852, Bull. No. 37, September 17, 1973.
19. V.V. Pokasov, V.A. Tartakovsky, A.G. Selivanov, O.N. Emaleev, and V.P. Lukin, "*The tracing phase meter in the optical range*," Inventor's Certificate No. 664118, Bull. No. 15, May 25, 1979.